Formation of Liquid Bridges Between Porous Matrix Blocks

Morteza Dejam
Dept. of Chemical and Petroleum Engineering, Sharif University of Technology, Tehran, Iran

Hassan Hassanzadeh
Dept. of Chemical and Petroleum Engineering, Schulich School of Engineering, University of Calgary, Calgary, AB, Canada T2N 1N4

DOI 10.1002/aic.12262
Published online April 22, 2010 in Wiley Online Library (wileyonlinelibrary.com).

It is widely accepted that, in fluid flow and transport in fractured porous media, there exists some degree of block-to-block interaction that may lead to capillary continuity. The formation of liquid bridges causing interaction between blocks will affect oil recovery from naturally fractured reservoirs. However, the accurate modeling of the growth and detachment of liquid bridges that may cause capillary continuity between matrix blocks remains a controversial topic. In an attempt to improve our understanding of the problem, a mechanistic model is developed in this work for the formation of liquid bridges between porous blocks. The proposed model considers growth and detachment of pendant liquid droplets perpendicular to the horizontal and smooth fracture between porous matrix blocks. The liquid bridge model is then coupled with various upscaled fracture capillary pressure models to study the liquid bridge formation process. An expression is obtained that relates the commonly used fracture capillary pressure to the critical length of the liquid element. Results based on various fracture capillary pressure models reveal that the threshold Bond number is an important parameter in the formation of liquid bridges. We introduce a simple mechanistic model for the formation of liquid bridges in a horizontal fracture between two porous blocks, advancing our understanding of the two-phase flow in fractured porous media.
 AIChE J, 57: 286–298, 2011
Keywords: liquid bridge, capillary continuity, fracture capillary pressure, mathematical modeling, fractured porous media

Introduction

Warren and Root[1] developed an analytical solution for single-phase, transient and radial flow in fractured porous media. They also presented an equation for the shape factor for matrix blocks within an orthogonal fracture system. Their double porosity model assumes a continuous uniform fracture network oriented parallel to the principal axis of the permeability. The matrix blocks in this system occupy the same physical space as the fracture network, and are assumed to have no communication between the matrix blocks.[1] This assumption is the main drawback in their theory; because, in reality, there exists some degree of block-to-block interaction. The interaction between the porous matrix blocks, which has a strong effect on oil recovery as well as the oil flow rate in fractured porous media, needs to be considered to have a reliable prediction of the reservoir performance.[2]

Later, the single-block concept was introduced in the simulation of fractured petroleum reservoirs.[3] The single-block concept assumes that the matrix blocks drain independently;

Correspondence concerning this article should be addressed to H. Hassanzadeh at hhassanz@ucalgary.ca.

therefore, the performance of stack blocks is equal to the performance of a single block multiplied by the number of individual blocks. The interaction between matrix blocks has been suggested by Saidi et al.[3] They attributed the interaction between porous matrix blocks to the reinfiltration process and capillary continuity between the adjacent matrix blocks through liquid bridges; however, the interaction between the matrix blocks by reinfiltration was the major theme of their study.[3]

Saidi[2] assumed capillary discontinuity between a stack of matrix blocks and argued that, if the fracture aperture is about 50 μm or more, capillary continuity between a stack of matrix blocks cannot be imagined. Saidi[2] also argued that capillary continuity between a stack of matrix blocks through liquid bridges can be envisioned if the fracture aperture is about 10 μm or less.[2] Horie et al. experimentally showed that if strong capillary continuity exists between the adjacent matrix blocks, it makes an appreciable increase in the recovery from fractured porous media.[4]

Firoozabadi and Hauge[5] and Labastie[6] have addressed the challenges in accurate prediction of naturally fractured reservoirs performance. Firoozabadi and Markeset experimentally showed that fracture-liquid transmissibility, incorporating both fracture gas–oil capillary pressure and fracture-liquid relative permeability, causes the high liquid pressure drop across the fractures.[7] This pressure drop governs the liquid film flow in a fracture between two matrix blocks, which significantly affects the recovery from a stack of matrix blocks.[7,8]

Dindoruk and Firoozabadi, therefore, modeled liquid film flow through a single liquid bridge using a boundary integral method to find the relationship between fracture capillary pressure, fracture-liquid permeability, and the shape of liquid bridge.[8] They concluded that the liquid bridge interface in a horizontal fracture has a circular shape at small capillary number.[8] Later, Firoozabadi and Markeset demonstrated that capillary continuity is maintained between two blocks, even in the presence of partially impermeable spacers in the fractures.[9]

Aspenes et al. used magnetic resonance imaging (MRI) to monitor fluid saturation variations in both the matrix and the fractures.[10] They concluded that the size of the bridges is controlled by the rock wettability and not by the pressure difference applied across the fracture. In other words, they found that wetting phase bridges establish the capillary continuity across the fracture between matrix blocks.[10]

Little attention has since been given on the formulation of the formation, growth, and detachment of liquid bridges causing capillary continuity between matrix blocks; and, this problem still remains a controversial topic. This work is an effort to improve our understanding of the conditions at which a liquid bridge can be expected to form between two porous matrix blocks.

Hoteit and Firoozabadi recently introduced a new approach for the modeling of multi-phase flow in fractured media.[11,12] In this new method, the concept of dual-porosity modeling has been put aside, due to its inherent limitations; and, gravity and capillarity are accounted for both in the fractures and matrix blocks using higher order numerical schemes. In this approach, they used a discrete-fracture model, where the fracture entities in the permeable media are described explicitly in a computational grid.

To address the capillary pressure contrast and saturation discontinuity in heterogeneous and fractured permeable media, they proposed a new consistent formulation in three dimensions, where the total velocity is expressed in terms of the wetting phase potential gradient and the capillary potential gradient. In this formulation, the coefficient of the wetting phase potential gradient is formulated in terms of the total mobility, which is smoother than the wetting phase mobility in the numerical modeling of two-phase immiscible flow in heterogeneous permeable media.[11,12]

Naturally fractured reservoirs consist of two media, namely a matrix with high storage volume and low permeability; and a fracture with low storage volume and high permeability. Performance forecasting for such reservoirs depends on the fracture system and the degree of block-to-block interactions. When oil is draining from an upper block into the lower fracture via an open face, it tends to flow downwards in a liquid film along the outflow face of that upper porous matrix block. When the film becomes thick enough it tends to deform and gradually forms pendant droplets.

In the case of a small fracture aperture, the surface of the adjacent lower porous matrix block easily makes contact with the droplets; and, a liquid bridge between two blocks is formed, which may cause capillary continuity between the upper and lower matrix blocks. This block-to-block continuity is one of the main phenomena affecting the oil recovery of naturally fractured reservoirs. On the other hand, if the fracture aperture is greater than a critical value, oil moves downward in the form of oil detached droplets or liquid elements.[2,13]

The role of facture aperture size on the formation of liquid bridges between porous matrix blocks in the presence of fracture capillary pressure is, however, not well understood.

In this study, a mechanistic model for the growth and detachment of a liquid element is developed to determine the critical length of the detached liquid elements; and, the formation of liquid bridges between porous matrix blocks is investigated. This model is then coupled with various fracture capillary pressure models to examine the interplay of fracture capillary pressure and the block-to-block interaction process. This simple mechanistic model improves our understanding of immiscible flow in naturally fractured reservoirs within the conventional framework of dual porosity modeling of fluid flow in naturally fractured reservoirs.

Ghezzehei and Or and Or and Ghezzehei presented a model for liquid fragmentation and intermittent flow regimes inside inclined fractures for a given steady input flux.[14,15] Although the developed model herein is primarily based on the approach of Ghezzehei and Or,[14] the conditions considered in this study are completely different from those studied by Ghezzehei and Or.[14] In our work, the formation, growth, and detachment of liquid elements are considered to be perpendicular to the horizontal fracture between matrix blocks with a constantly fed flux from the upper porous matrix block, whereas Ghezzehei and Or[14] modeled the liquid bridges along the inclined fractures, especially vertical ones, with a steadily fed flux along the fracture.

Ghezzehei and Or[14] and Or and Ghezzehei[15] have shown that the traveling velocity and distance, due to the formation of discrete liquid elements, are considerably higher than

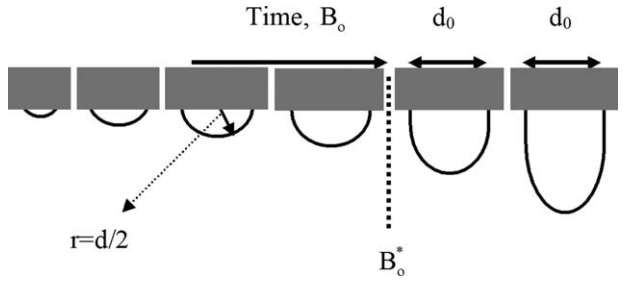

Figure 1. Growth and elongation of a liquid element attached to a feeding spot in which the Bond number increases with time.[14]

The liquid element begins to elongate when $B_o > B_o^*$.[14]

those due to continuum liquid film flow on both fracture walls. In addition, the primary focus of the Ghezzehei and Or[14] and Or and Ghezzehei[15] investigations was to study the potential for more rapid arrival times of pollutant carried along the fracture with discrete liquid bridges.

Our focal point, on the other hand, is the study of the potential for formation of liquid bridges, which may affect the mass transport mechanisms from a stack of blocks. Liquid bridges can strongly influence the two-phase gas–liquid flow in fractured porous media and affect capillary continuity. They may also have a major role in establishing the paths for the flow of drained oil through the horizontal fractures and, thus, oil recovery. Therefore, the creation of liquid bridges between porous matrix blocks becomes an important factor in oil production by gravity drainage. The formation of capillary continuity between blocks is related to the length of detached liquid elements, and the parameters that influence this length are investigated.

In the following section, we present the theoretical considerations of the formation, growth, and detachment of liquid elements.

Theoretical Modeling

This section describes a conceptual model for the elongation and subsequent breakup of a liquid element suspended from a horizontal surface beneath a porous matrix block. First, the Bond number and its critical value, after which the liquid element base diameter remains fixed and elongation occurs, is defined for liquid elements that are suspended vertically from the surface. The dynamics of liquid element elongation and breakup are described in the following subsections, using Wilson's one-dimensional viscous extension model. This model is then generalized to account for the dynamic capillary pressure effect.

Fundamental concepts

Let us assume a droplet is attached to a horizontal surface underneath a porous matrix block, as shown in Figure 1. A useful scaling of the importance of the gravitational force relative to the capillary force acting on the liquid element is known by the dimensionless Bond number given by:

$$B_o = \frac{\rho g r^2}{\sigma \cos\theta} \tag{1}$$

where σ is the surface tension of the liquid–gas interface, θ is the dynamic contact angle, ρ is the liquid density, g is the gravitational acceleration, and r is the radius of the semicircular liquid element.

The dynamic Bond number varies with time until it reaches a threshold value. The threshold Bond number, B_o^*, of the liquid element, after which its base diameter (d_0) remains constant and elongation begins, can be defined as[14]:

$$B_o^* = \frac{\rho g r_0^2}{\sigma}. \tag{2}$$

The dynamic contact angle controls the early growth of the suspended droplet. Ghezzehei and Or[14] matched the diameters calculated at different conditions for the flow of traveling liquid elements along the inclined fractures with the measured values from experiments. With such experimental measurements, they obtained an estimation of the threshold Bond number: $B_o^* = 0.05$ for an air–water system.[14] A similar order of the threshold Bond number was identified in the experiments of Prazak et al., giving rise to an intermittent flow regime in packs of coarse sand.[16]

The dynamic contact angle is given by the so-called Hoffman-Voinov-Tanner law for small capillary numbers by[17–19]:

$$\theta \cong \sqrt[3]{\theta_e^3 + c_T Ca} \tag{3}$$

where

$$Ca = \frac{\mu U_0}{\sigma} \tag{4}$$

and is the capillary number; μ is the liquid viscosity; U_0 is the interface velocity; θ_e is the static (equilibrium) contact angle; and C_T is a numerical coefficient, which was given by Hoffman[17] to be about 72, with some dependence on the flow system size.[17–19] The dynamic contact angle controls the early development and shape of the interface. The static contact angle can be considered as zero for a strong wetting liquid, and the dynamic contact angle can be approximated by $\theta = (c_T Ca)^{1/3}$.

In the following subsections, we model the elongation and subsequent breakup of an incompressible liquid element. First, the one-dimensional model of Wilson[20] is used to obtain a relationship for the critical length of an elongated liquid element at the breakup. A more generalized form of the elongation model is then presented by incorporation of the dynamic capillary pressure for a suspended liquid element from a horizontal surface.

Extension and detachment of a free liquid element

We are primarily interested in the elongation and subsequent breakup of a liquid element suspended from a horizontal surface, which is bounded by curved gas–liquid interfaces. We assume that the associated Bond number is larger than the threshold Bond number, B_o^*, after which the base diameter remains constant. The dynamic contact angle is important during the early growth of the liquid element, and its effect is discussed in the next subsection.

We assume an axisymmetric circular element of an incompressible and Newtonian fluid extruded from a feeding spot,

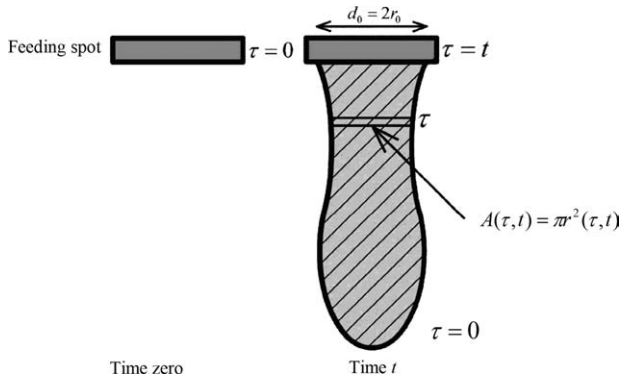

Figure 2. Wilson approach to model extension and detachment of a free liquid element.[20]

as shown in Figure 2. The liquid element has a cross-sectional area, A, and is fed by a steady volumetric flux, Q, from the top. It is convenient to use a Lagrangian coordinate system, where the emerging fluid particles are marked by time, τ, at the present time, t, in which $0 \leq \tau \leq t$. Under such a condition, $\tau = 0$ corresponds to bottom end of the liquid element, and $\tau = t$ is the location of the liquid particle emerging at the present time. Assuming $Z(\tau,t)$ is the distance below the feed point of the dripping liquid element, a mass balance between τ and $\tau + \Delta\tau$ in a Lagrangian coordinate system gives[20]:

$$A\frac{\partial Z}{\partial \tau} = -Q. \tag{5}$$

Using the mass balance given by Eq. 5, a force balance on the liquid element gives[20]:

$$-\left(3\mu\frac{1}{A}\frac{\partial A}{\partial t}+\frac{\sigma}{r}\right)A + 2\pi r\sigma = \rho g Q\tau \tag{6}$$

where $-(3\mu\partial A/\partial t+\sigma A/r)$ is the net longitudinal force, $2\pi r\sigma$ is the surface tension force, and $\rho gQ\tau$ is the gravity force.[20] The parameter 3μ is the elongational viscosity or the Trouton expression, which is three times the shear viscosity for a Newtonian fluid; and, the term $\sigma A/r$ includes the surface tension effect as a source of stress on the liquid element.[20–22] The detailed analytical solution to the above equation is reported by Wilson,[20] as described in the Appendix.

In the following subsection, we use this solution to find the critical length of the liquid element for our application of interest.

When the liquid element is unable to support its own weight, a narrow neck forms and eventually breaks, releasing a liquid droplet. The liquid element in this condition is called the critical liquid element, τ_c. The dimensionless form of τ_c is given by[20]:

$$\tau_{Dc} = \frac{2}{\delta}\left[\frac{\tau_{Dc}}{3\delta}\ln\left(\frac{\tau_{Dc}-3\delta}{\tau_{Dc}}\right)+\frac{\tau_{Dc}}{\tau_{Dc}-3\delta}\right] \tag{7}$$

where $t_D = t/(\mu A_0/\rho gQ)^{1/2}$, $\tau_D = \tau/(\mu A_0/\rho gQ)^{1/2}$, $A_D = A/A_0$, and $\delta = (\pi/9\mu\rho gQ)^{1/2}$, as defined by Wilson.[20] The dimensionless parameter, δ, can be expressed as a function of system dimensionless numbers as given by:

$$\delta = \frac{1}{3}(B_o^* Ca)^{-1/2}. \tag{8}$$

If we substitute for τ_{Dc} given by Eq. 7 into Eq. A4 of the Appendix, the following relationship can be obtained between τ_{Dc} and τ_{Dc}:

$$\tau_{Dc} = \frac{6}{t_{Dc}} + 3\delta. \tag{9}$$

The critical time given by Eq. 7 is an implicit function of δ and cannot be used directly in the analysis that follows. Therefore, one needs to solve the nonlinear equation to find the behavior of τ_{Dc} as a function of the dimensionless group δ. For our application of interest, δ is larger than one and can be approximated as:

$$\tau_{Dc} \approx 3\delta + 1 \quad \text{for } \delta > 1. \tag{10}$$

Figure 3 shows τ_{Dc} as a function of δ, as compared with the exact form of Eq. 7. Using the dimensional parameters defined, the dimensional form of τ_{Dc} is given by:

$$\tau_c \approx \left(\frac{\mu A_0}{\rho gQ}\right)^{1/2}\left[1+3\sigma\left(\frac{\pi}{9\mu\rho gQ}\right)^{1/2}\right]. \tag{11}$$

The mass of the detached liquid element can be calculated by $M_c = \rho Q\tau_c$, that is,

$$M_c \approx \rho Q\left(\frac{\mu A_0}{\rho gQ}\right)^{1/2}\left[1+3\sigma\left(\frac{\pi}{9\mu\rho gQ}\right)^{1/2}\right]. \tag{12}$$

Assuming a cylindrical liquid element with an average cross-sectional area of $A \approx \pi r_0^2$, the mass of the liquid

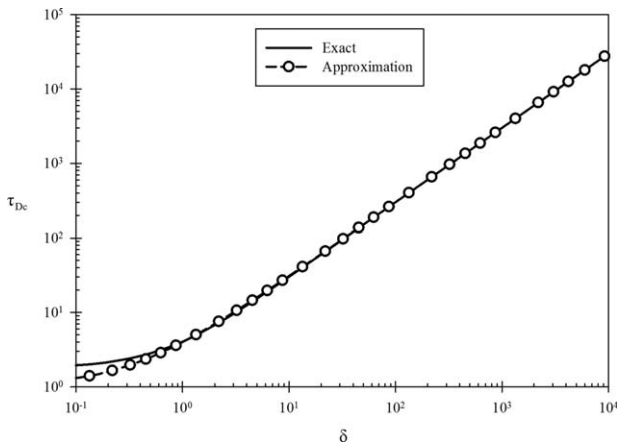

Figure 3. Comparison between exact and approximate solutions for τ_{Dc} vs. δ (Eqs. 7 and 10, respectively).

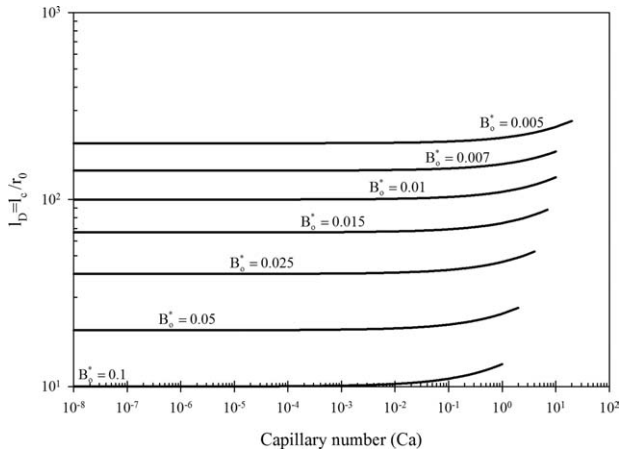

Figure 4. The critical dimensionless length of the liquid element as a function of the capillary number for different values of the threshold Bond number (Eq. 13).

element can be expressed by $M_c = \rho l_c \pi r_0^2$. Using Eq. 12, we can estimate the dimensionless critical length of the liquid element, $l_D = l_c/r_0$, by:

$$l_D \approx \frac{1}{B_o^*}[1 + \sqrt{B_o^* Ca}]. \tag{13}$$

Figure 4 shows the critical dimensionless length of the liquid element, as a function of the capillary and the threshold Bond numbers. The results reveal the critical length of the liquid element is nearly independent of the capillary number for $Ca <\sim 0.1$. On the basis of capillary-controlled displacements, viscous forces are considered to be negligible, that is, $Ca < 10^{-6}$.[23–28] Also, the threshold Bond number has an approximate value of 0.0125–0.05.[14,16] For the application of interest, the dimensionless group $B_o^* Ca$ is, therefore, usually much smaller than one ($B_o^* Ca < 5 \times 10^{-8}$); thus, $(B_o^* Ca)^{1/2} 1$ (or $\delta \gg 1$), and it is possible to approximate the critical length of the detached liquid element by $l_D = 1/B_o^*$.

In this section, we have ignored the effect of dynamic capillary pressure during the elongation and subsequent detachment of the liquid element. In the following subsection, a generalized model is presented where the effect dynamic capillary pressure is included; and, the results are compared with those of the former case.

Generalized form of the extension and detachment model

In the absence of surface tension forces, the governing equation for elongation of the suspended liquid element can be expressed by[14,20]:

$$-3\mu \frac{\partial A(\tau,t)}{\partial t} = \rho g Q \tau. \tag{14}$$

This equation implies that the cross-sectional area of the liquid elements contracts at a rate proportional to the weight of liquid element, $\rho g Q \tau$. An important force associated with surface tension, which balances part of the liquid element weight, is the force resulting from the capillary pressure. Using this notion, Ghezzehei and Or generalized Wilson's[20] viscous elongation model (Eq. 14) to take into account the capillary forces, to study the liquid fragmentation within vertical and inclined fractures.[14] We use a similar concept and incorporate capillary pressure forces to generalize the base viscous elongation model (Eq. 14) for our application of interest. This model is then used to investigate the effect of dynamic capillary pressure on the elongation and subsequent detachment of a liquid element suspended from a horizontal plane.

The static and dynamic capillary pressure forces can be represented by $p_{cs} = 2\sigma/r$ and $p_{cd} \sim (\sigma/r)Ca^{2/3}$, respectively.[29–31] The experimental data of Weitz et al.[29] shows a scaling in the form of $p_{cd} \sim Ca^{0.5\pm0.1}$ for the dynamic capillary pressure in porous media. In the following analysis, we use a similar scaling to account for the dynamic character of the capillary forces. Applying the static and dynamic capillary pressure contributions in the force balance of Eq. 14, we obtain:

$$-3\mu \frac{\partial A(\tau,t)}{\partial t} - \frac{\sigma A(\tau,t)}{r} + 2\pi r\sigma + \frac{\sigma A(\tau,t)}{r}\beta Ca^{2/3} = \rho g Q \tau. \tag{15}$$

Using the previously defined dimensionless variables and simplifying, results in:

$$\frac{\partial A_D}{\partial t_D} - \delta(1 + \beta Ca^{2/3})\sqrt{A_D} = -\frac{1}{3}\tau_D \tag{16}$$

where $t_D = t/(\mu A_0/\rho g Q)^{1/2}$, $t_D = \tau/(\mu A_0/\rho g Q)^{1/2}$, $A_D = A/A_0$, $\delta = \sigma(\pi/9\mu\rho g Q)^{1/2}$, and β is a constant of the order of 10 for a sliding liquid slug in a capillary tube.

Equation 16 is similar to Eq. A1, presented in the Appendix, given by Wilson[20] for the slow dripping of a viscous liquid with an extra term, $\beta Ca^{2/3}$, to account for the dynamic behavior of the capillary pressure. The related initial condition in dimensionless form is similar to the previous case, as given by:

$$A_D = 1 \quad @\ t_D = \tau_D. \tag{17}$$

The analytical solution for the differential equation given by Eq. 16, subject to the initial condition (Eq. 17), is given by:

$$t_D = \tau_D + \frac{2}{\delta(1+\beta Ca^{2/3})}\left[A_D^{1/2} - 1 + \frac{\tau_D}{3\delta(1+\beta Ca^{2/3})} \ln\left(\frac{3\delta(1+\beta Ca^{2/3})A_D^{1/2} - \tau_D}{3\delta(1+\beta Ca^{2/3}) - \tau_D}\right)\right]. \tag{18}$$

If we put $A_D = 0$, it is possible to find a relation between t_D and τ_D when the cross-sectional area approaches zero. Using the critical values for t_D and τ_D, we have:

$$t_{Dc} = \tau_{Dc} - \frac{2}{\delta(1+\beta Ca^{2/3})}\left[1 + \frac{\tau_{Dc}}{3\delta(1+\beta Ca^{2/3})}\ln\left(\frac{\tau_{Dc} - 3\delta(1+\beta Ca^{2/3})}{\tau_{Dc}}\right)\right]. \quad (19)$$

For a constantly fed flux from the top and an incompressible liquid, when the cross-sectional area goes to zero, its length approaches infinity, suggesting that the velocity of a liquid particle, $d\tau_{Dc}/dt_{Dc}$ goes to infinity. Therefore, we can write:

$$\frac{dt_{Dc}}{d\tau_{Dc}} = 1 - \frac{2}{\delta(1+\beta Ca^{2/3})}\left[\frac{1}{3\delta(1+\beta Ca^{2/3})}\ln\left(\frac{\tau_{Dc} - 3\delta(1+\beta Ca^{2/3})}{\tau_{Dc}}\right) + \frac{1}{\tau_{Dc} - 3\delta(1+\beta Ca^{2/3})}\right] = 0. \quad (20)$$

Solving this equation results in a relationship between τ_{Dc} and δ:

$$\tau_{Dc} = \frac{2}{\delta(1+\beta Ca^{2/3})}\left[\frac{\tau_{Dc}}{3\delta(1+\beta Ca^{2/3})}\ln\left(\frac{\tau_{Dc} - 3\delta(1+\beta Ca^{2/3})}{\tau_{Dc}}\right) + \frac{\tau_{Dc}}{\tau_{Dc} - 3\delta(1+\beta Ca^{2/3})}\right]. \quad (21)$$

If we back substitute for τ_{Dc} given by Eq. 21 into Eq. 19, the following relationship can be obtained relating τ_{Dc} and t_{Dc}:

$$\tau_{Dc} = \frac{6}{t_{Dc}} + 3\delta(1+\beta Ca^{2/3}). \quad (22)$$

Similar to the previous case without the dynamic capillary effect, Eq. 21 shows that the critical time and the dimensionless group, $\delta(1 + \beta Ca^{2/3})$, are related in an implicit fashion and cannot be used directly. Therefore, one needs to solve nonlinear Eq. 21 to find the behavior of τ_{Dc} as a function of the dimensionless group. Again, it is more suitable to approximate Eq. 21 for large values of δ as in the application of our interest:

$$\tau_{Dc} \approx 1 + 3\delta(1+\beta Ca^{2/3}) \quad \text{for } \delta(1+\beta Ca^{2/3}) > 1. \quad (23)$$

The mass of the detached liquid element ($M_c = \rho Q \tau_c$) can be obtained by:

$$M_c \approx \rho Q\left(\frac{\mu A_0}{\rho g Q}\right)^{1/2}\left[1 + 3\sigma\left(\frac{\pi}{9\mu\rho g Q}\right)^{1/2}(1+\beta Ca^{2/3})\right]. \quad (24)$$

A comparison of Eqs. 24 and 12 reveals that the dynamic capillary pressure adjusts the mass of the detached liquid element. Assuming a cylindrical liquid element with an average cross-sectional area of $A \approx \pi r_0^2$, the mass of the detached liquid element can be expressed by $M_c = \rho l_c \pi r_0^2$; and, the dimensionless critical length of the liquid element, $l_D = l_c/r_0$, is given by:

$$l_D \approx \frac{1}{B_o^*}[1 + \sqrt{B_o^* Ca} + \beta Ca^{2/3}]. \quad (25)$$

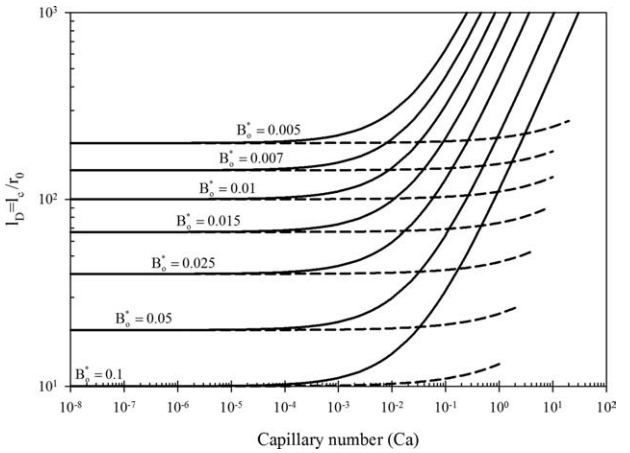

Figure 5. The critical dimensionless length of the liquid element as a function of the capillary number for different values of the threshold Bond number (Eq. 25, solid lines).

Dashed lines are drawn based on Eq. 13, which does not include the effect of forces related to the dynamic contact angle.

Figure 5 shows the critical dimensionless length of the liquid element as a function of the capillary and Bond numbers (solid lines). For comparison, this figure also illustrates the results of the previous case, which did not take into consideration the dynamic capillary effect (dashed lines). The results show that, as anticipated, for a particular capillary number, by increasing the threshold Bond number, the length of the detached liquid element decreases. In addition, for a specific threshold Bond number, the critical dimensionless liquid element length increases by increasing the capillary number.

The results demonstrate that the critical length of the detached liquid element is nearly independent of the capillary number for $Ca <\sim 10^{-4}$, as opposed to $Ca <\sim 0.1$ without the effect of the dynamic capillary pressure. Furthermore, at large capillary numbers, the dynamic capillary pressure effect can support the mass of a larger liquid element, as compared with the previous case where this effect was ignored.

Similar to the previous case for a capillary dominated system ($Ca < 10^{-6}$),[23–28] the dimensionless group, $B_o^* Ca$, is usually much smaller than one ($B_o^* Ca < 5 \times 10^{-8}$). Therefore, for such a system, $(B_o^* Ca)^{1/2} + \beta Ca^{2/3} << 1$, and we may obtain a fairly accurate critical length of the detached liquid element by using $l_D = 1/B_o^*$. Ghezzehei and Or[14] used the dynamic capillary model of Bico and Quere[31] to include the force related to dynamic contact angle into their

formulation. As a result of the matching between the proposed model and the measured experimental data, they concluded that the force related to the dynamic contact angle does not play a significant role in determining the volume and mass of the detached liquid element.[14]

In the following section, we couple the model developed in this section with various fracture capillary pressure models to study the block-to-block interaction in fractured porous media.

Fracture Capillary Pressure Models

It is believed that there exists some degree of block-to-block interaction that may lead to capillary continuity in naturally fractured reservoirs; therefore, capillary pressure in the fracture may play a major role in the establishment of capillary continuity between matrix blocks. In the previous section, we developed a relationship for the length of liquid element at the onset of detachment. The developed model is primarily based on a capillary pressure for a pendant droplet from a horizontal surface (bottom of the upper matrix block), not for a fracture with a particular aperture.

The intention of this section is to relate the developed onset length of the liquid element to the capillary pressure inside two parallel plates with a particular aperture. Obviously, if the length of the detached liquid element is larger than the fracture aperture, a liquid bridge may be established. On the other hand, if the length of the element is smaller than the fracture aperture, a liquid bridge does not form. Therefore, the thickness (aperture) of the horizontal fracture determines the possibility of the existence of liquid bridges. Stable liquid bridges may have a major role in establishing the paths for the bulk flow of drained oil through the horizontal fracture.

The fracture capillary pressure is often used as a matching parameter, when considering the effect of horizontal fracture on the flow rate and recovery of oil from the stack of blocks. In a continuum scale, a fracture is a part of the stack of blocks where there is a pressure difference between the gas and oil phases inside the fracture. However, the physics of this capillary pressure and how it affects the gravity drainage mechanism need to be addressed.

Zero fracture capillary pressure ($p_{cf} = 0$) has been widely hypothesized in the numerical simulation of fractured reservoirs, but it does not have a sound basis.[4] A modified Laplace equation has also been used to relate the capillary pressure in a fracture to the fracture aperture, that is, $p_{cf} = 2\sigma\cos\theta/b$[13,32]; however, this equation was originally derived for the case of the flow parallel to the fracture surface, not perpendicular to it.[33] Horie et al. are among those who used this relation for the determination of the fracture capillary pressure.[4] Firoozabadi and Hauge showed that, due to the fracture roughness, the fracture capillary pressure is neither zero nor a constant value, but it is a function of the oil saturation in the fracture.[5]

Previous studies of the fracture capillary pressure have been mainly used for the horizontal fracture properties (i.e., fracture aperture and type of spacers). Rossen and Shen argued that pseudo capillary pressure curves for both the porous matrix and the fracture are able to represent the behavior of fractured porous media.[34] Quandalle and Sabathier assumed zero fracture capillary pressure; however, in a test case, they made it non-zero, to match the experimental and numerical results.[35]

Sajjadian et al.[13] emphasized that, when the fracture aperture was more than a critical value, the fracture capillary pressure may be considered zero. When the fracture aperture is less than the critical value, the fracture capillary pressure is related to saturation profiles inside the porous matrix blocks (i.e., the existence of oil continuous path), as well as the height of the fracture from the gas–oil contact (GOC) in the neighboring vertical fractures.[13]

Reitsma and Kueper[36] developed a laboratory method to measure the drainage and imbibition capillary pressure curves for a single, rough-walled fracture in limestone, using oil and water as the non-wetting and wetting phases, respectively. The method includes a loading system and a designed capillary barrier to the non-wetting phase, which has three important roles in the experiment: (1) to prevent the flow of the non-wetting phase across the barrier, (2) to allow for fracture closure, and (3) to provide a good hydraulic connection of the wetting phase in the fracture with external pressure control.

A vertically mounted burette on a gauge point containing water was used to measure the volume of wetting fluid entering and exiting the fracture via the capillary barrier. The point gauge allowed for accurate measurement of the capillary pressure, as well as precise adjustment of the wetting phase pressure in the fracture through vertical movement of the burette. To measure the drainage capillary pressure, the burette was lowered incrementally, thereby increasing the fracture capillary pressure. After reaching equilibrium, the amount of wetting fluid removed from the fracture, corresponding to each fracture capillary pressure, was recorded. Using this procedure, they were able to measure an imbibition capillary pressure curve, starting at any point on the drainage curve, by incrementally raising the burette.[36]

Reitsma and Kueper[36] used the models of Brooks and Corey[37] and van Genuchten[38] to model experimental results of the fracture capillary pressure vs. saturation in a drainage process. The Brooks–Corey model for the application of interest is given by[36,37]:

$$p_{cf} = p_d \left(S_e\right)^{-1/\lambda} \tag{26}$$

where p_d is the entry pressure and λ is a pore size distribution index. S_e is an effective saturation given by:

$$S_e = \frac{S_{of} - S_{orf}}{1 - S_{orf}} \tag{27}$$

where S_{of} is the fracture oil saturation and S_{orf} is a curve-fitting parameter intended to represent the irreducible oil saturation in the fracture.[36,37]

The van Genuchten[38] model for the application of interest is presented by[36,38]:

$$p_{cf} = p_o \left(S_e^{-1/m} - 1\right)^{1/n} \tag{28}$$

where m, n, and p_o are fitting parameters and S_e is presented by:

$$S_e = \frac{S_{of} - S_{orf}}{S_{osf} - S_{orf}} \tag{29}$$

S_{osf} is the fracture oil saturation at a capillary pressure equal to zero. In this application, S_{osf} is equal to 1 and Eq. 29 reduces to Eq. 27.[36,38]

The following equation gives the Mualem's model for unsaturated flow[39]:

$$n = (1 - m)^{-1}. \tag{30}$$

The measured relationship between capillary pressure and fluid saturation was found to be well presented by a Brooks–Corey model.[36,37]

Dindoruk and Firoozabadi proposed a model of fracture capillary pressure, as a function of liquid saturation in the fracture, as given by[40]:

$$p_{cf} = p_{cf}^0 + \sigma_f \left[\ln\left(\frac{S_{of} - S_{orf}}{1 - S_{orf}} \right) \right]^{n_f}, \quad p_{cf} \geq p_{cf}^0 \tag{31}$$

where n_f is a constant and p_{cf}^0, σ_f and S_{orf} are the fracture threshold capillary pressure, the coefficient of fracture capillary pressure curve, and the residual oil saturation in the fracture space, respectively. This model, assumes that the fracture capillary pressure curve has a shape similar to that of a porous medium, but with major differences in its curvature.[40]

As mentioned by Horie et al.,[4] it is reasonable for the fracture to have a very low irreducible wetting phase saturation of oil, compared with the residual oil saturation in the porous matrix block. The consequence of assuming a saturation dependent fracture capillary pressure is that the capillary continuity between a stack of porous matrix blocks may be expected.[4] The parameters p_{cf}^0 and σ_f in Eq. 31 are adjustable parameters to be determined from history matching of data.[40]

Interplay of fracture capillary pressure and liquid bridge formation

In a previous section, a relationship was developed for the length of the suspended liquid at the onset of detachment. As mentioned earlier, if the suspended liquid from the upper surface detached before touching the lower block, a liquid bridge does not form, and the detached liquid reinfiltrates into the lower block. However, if the suspended liquid element touches the lower surface, a liquid bridge forms, which may lead to a block-to-block interaction. In this case, once the extended liquid element touches the top surface of the lower matrix block, as shown in Figure 6, the fracture capillary pressure can be written by[14,41]:

$$p_{cf} \approx \sigma \left(\frac{1}{r_0} - \frac{2\cos\theta}{b} \right), \quad p_{cf} \geq 0 \tag{32}$$

where b is the fracture aperture and $r_0 = d_0/2$ and is the radius of the liquid element.

The length of the liquid element at the onset of liquid bridge formation (when the liquid element touches the lower surface) is identical to the fracture aperture ($l_c = b$). Therefore, using Eqs. 25 and 32 and eliminating r_0, the critical length of the liquid element leading to a liquid bridge can be expressed by:

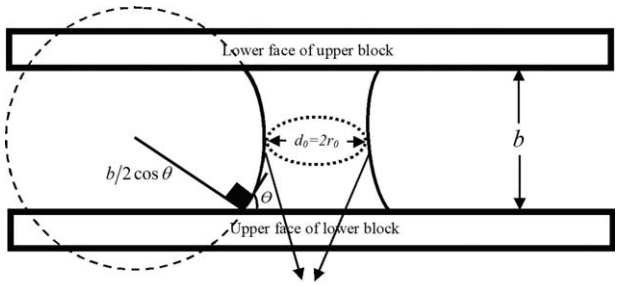

Figure 6. Formation of a liquid bridge between upper and lower porous matrix blocks.

$$l_c = \frac{\sigma}{p_{cf}} \left(\frac{[1 + \sqrt{B_o^* Ca} + \beta Ca^{2/3}]}{B_o^*} - 2\cos\theta \right). \tag{33}$$

As mentioned before, for the application of interest, $(B_o^* Ca)^{1/2} + \beta Ca^{2/3} \ll 1$; and, if we assume $\cos\theta = 1$, Eq. 33 turns into:

$$l_c = \frac{\sigma}{p_{cf}} \left(\frac{1}{B_o^*} - 2 \right). \tag{34}$$

The analysis presented above cannot be directly linked to reservoir simulation flow models; however, the fracture capillary pressure model used in flow simulations may be a proper way to relate this developed theory to flow models. In other words, the proper linkage between theory and the numerical flow models may be possible by accurate representation of the upscaled fracture capillary pressure in these models.

As mentioned earlier, various capillary pressure models have been reported in the literature; however, some of these models do not have a sound theoretical basis, and the related parameters have been used as matching parameters. For example, zero capillary pressure in the fractures has been used, without a clear understanding of how this parameter affects flow simulation accuracy and with no practical method for selecting alternate values. In the following subsections, we use commonly used fracture capillary pressure models that are available in the literature to investigate the effect of various parameters on liquid bridge formation in fractured porous media.

Zero fracture capillary pressure ($p_{cf} = 0$)

Zero fracture capillary pressure has been widely used in the simulation of fractured reservoirs. For this particular case, the capillary pressure in the fracture is independent of wetting phase saturation; and, Eq. 34 suggests that, when capillary forces diminish in the fracture ($p_{cf} \propto \sigma$, $\sigma \to 0$ or $B_o^* \to \infty$), the critical length of the liquid also goes to zero, implying that no liquid bridge formation is expected for this particular case. This also suggests that the common

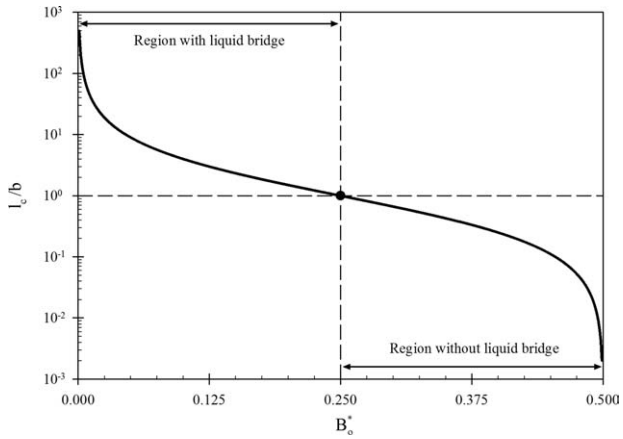

Figure 7. Illustration of the regions with and without liquid bridge formation for a constant fracture capillary pressure.

assumption of zero fracture capillary pressure in the simulation of fractured reservoirs may lead to erroneous predictions.

Constant fracture capillary pressure ($p_{cf} = 2\sigma/b = constant$)

For this case, substituting for the fracture capillary pressure in Eq. 34, we obtain:

$$\frac{l_c}{b} = \frac{1}{2}\left(\frac{1}{B_o^*} - 2\right). \tag{35}$$

The relationship obtained suggests that, if $l_c/b > 1$, the length of the liquid element before detachment is larger than the fracture aperture; and, the formation of a liquid bridge is expected. On the other hand, if $l_c/b < 1$, the liquid element detaches from the upper surface before reaching the lower block surface; and, consequently, no liquid bridge forms.

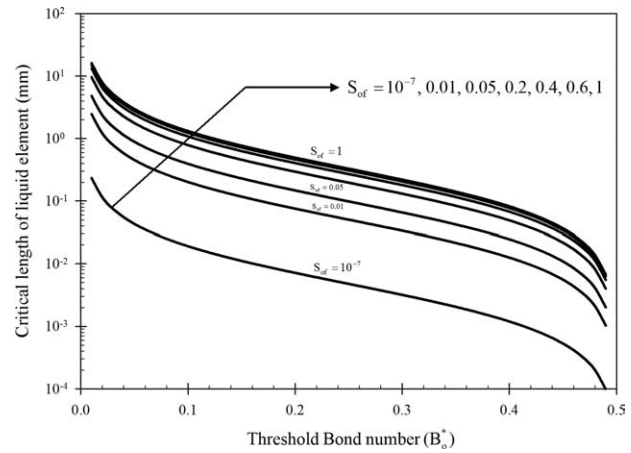

Figure 8. Critical length of the liquid element obtained based on the Dindoruk and Firoozabadi[40] model of the fracture capillary pressure, using data extracted from the work of Tan and Firoozabadi.[42]

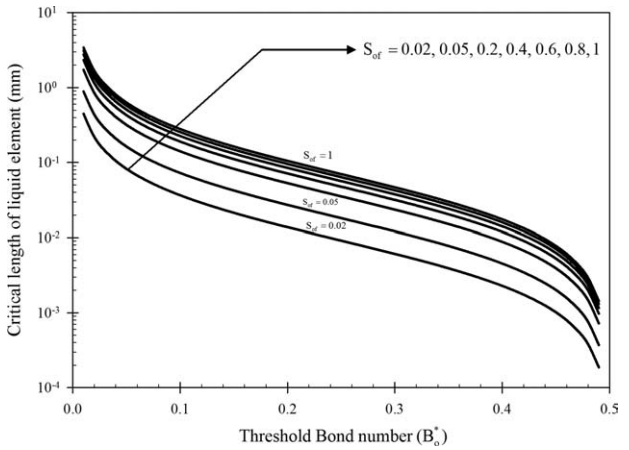

Figure 9. Critical length of the liquid element obtained using the Brooks–Corey[37] model, tuned with the experimental measurement of fracture capillary pressure by Reitsma and Kueper.[36]

Equation 35 shows that the critical threshold Bond number for the case of constant fracture capillary pressure is 0.25. Figure 7 shows the regions with and without liquid bridge formation.

Saturation dependent fracture capillary pressure [$p_{cf} = f(S_{of})$]

The two previous models for capillary pressure in a fracture do not provide information about the wetting phase saturation inside the fracture. It is more practical to relate the fracture capillary pressure in the fracture to the wetting phase saturation. Using Eq. 34, the critical length of the liquid element can be calculated. Figures 8–10 show the critical length of the liquid element at the onset of liquid bridge formation for different fracture oil saturations, based on Dindoruk and Firoozabadi,[40] Brooks–Corey,[37] and van Genuchten[38] models, respectively. Data used for the Dindoruk

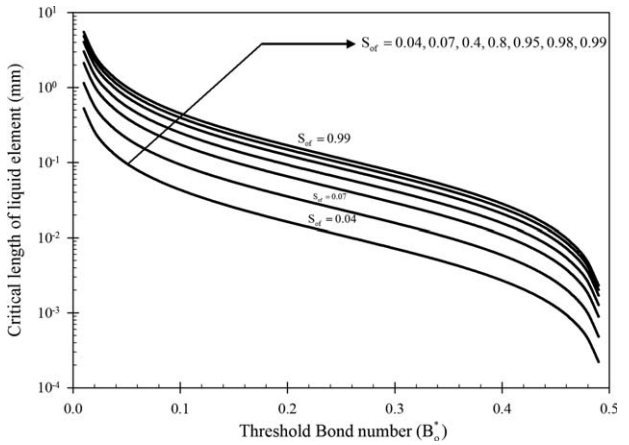

Figure 10. Critical length of the liquid element obtained using the van Genuchten[38] model, tuned with the experimental measurement of fracture capillary pressure by Reitsma and Kueper.[36]

Table 1. Data Used in Calculations of the Critical Length of the Liquid Element[4,36,42,43]

Parameter	Value
Oil-gas surface tension, σ (N/m)	0.01
Fracture threshold capillary pressure, p_{cf}^0 (Pa)	60.653
Coefficient of fracture capillary pressure curve, σ_f (Pa)	15.857
Residual oil saturation in the fracture for the Dindoruk and Firoozabadi, Brooks-Corey, van Genuchten models, respectively, S_{orf} (fraction)	0, 0.013, 0.039
Entry pressure, p_d (Pa)	285.331
Pore size distribution index, λ (dimensionless)	2.431
Fitting parameter, p_0 (Pa)	393.951
Fitting parameter, m (dimensionless)	0.816

and Firoozabadi[40] model were extracted from Tan and Firoozabadi[42]; whereas, for other models, the parameters were obtained from experimental measurements of fracture capillary pressure by Reitsma and Kueper.[36] The parameters of various fracture capillary pressure models are given in Table 1.[4,36,42,43]

Because the parameters used for the Brooks–Corey[37] and van Genuchten[38] models are calculated in such a way that both models match the same experimental data measured by Reitsma and Kueper,[36] the predictions of these models for the critical length of the liquid elements are close to each other. These predictions are different from those obtained by the Dindoruk and Firoozabadi[40] model, since their applied data were extracted from different sources. However, all models show the same trend for the critical length of liquid element vs. the threshold Bond number at various fracture oil saturations.

The results presented in Figures 8–10 show that, for a constant fracture oil saturation (or constant fracture capillary pressure), the critical length of liquid element decreases when the threshold Bond number increases. This implies a smaller critical length of the liquid element for a higher density difference between the wetting and non-wetting phases. The results also reveal that, for a constant fracture oil saturation and at high threshold Bond numbers, the critical length of the liquid element tends to zero, implying that a liquid bridge does not form. On the other hand, as the threshold Bond number tends to zero, the critical length of the liquid element approaches high values, suggesting that formation of a liquid bridge is possible.

Figure 11 shows the critical length of the liquid element as a function of fracture oil saturation for different capillary pressure models. A typical constant threshold Bond number of 0.05, reported by Ghezzehei and Or,[14] was used in this figure. The results show that, when oil saturation in the fracture increases, the critical length of the liquid element also increases. This is because, when the oil saturation in the fracture increases, the fracture capillary pressure, p_{cf}, decreases, leading to a larger critical length for the liquid element. This is also expected, because the critical length and thus the critical volume of the liquid elements reflect oil saturation in the fracture.

Saidi[2] argued that a fracture aperture of 50 μm or more is not sufficient to maintain capillary continuity via liquid bridges; however, he noted that capillary continuity between matrix blocks through liquid bridges can be envisioned if the fracture aperture is about 10 μm or less.

The results presented in Figure 11 show that, as expected, when oil saturation approaches the residual oil saturation, the critical length of the liquid element asymptotically goes to zero. The results also indicate that, when fracture oil saturation is just above the residual oil saturation, the critical length of the liquid element is above 10 μm, suggesting that a liquid bridge formation can be expected for fracture apertures below this limit.

The results also reveal that, for the fracture capillary pressure models with threshold capillary height (Dindoruk and Firoozabadi[40] and Brooks–Corey[37] models), the critical length of the liquid element reaches a finite value. On the other hand, for van Genuchten's[38] model, the critical length of the liquid element approaches infinity for an oil-saturated fracture.

The oil recovery process form a single matrix block in a naturally fractured reservoir may be divided into two periods of pre- and post-incidence of the capillary-gravity equilibrium. Before the capillary-gravity equilibrium is established, it is expected that the rate of gravity drainage from a stack of blocks is different for a system with liquid bridges, compared with a system draining oil by dripping. Liquid bridges can potentially maintain capillary continuity across the stack of blocks and result in a high liquid transmissibility, leading to higher gravity drainage rate. It has been shown that this process can only be sustained to the point of the capillary-gravity equilibrium of a single matrix block.[7]

Experimental observations of Firoozabadi and Markeset[7] revealed that desaturation beyond the capillary-gravity

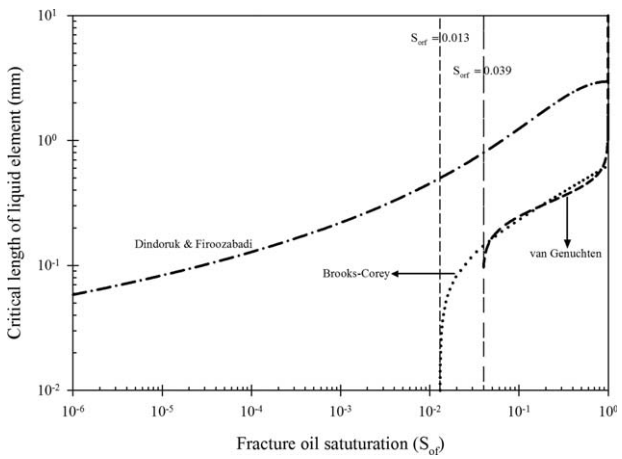

Figure 11. Critical length of the liquid element as a function of fracture oil saturation for the Dindoruk and Firoozabadi,[40] Brooks–Corey,[37] and van Genuchten[38] models of the fracture capillary pressure at a constant threshold Bond number of 0.05: the parameters of the Dindoruk and Firoozabadi[40] model were extracted from Tan and Firoozabadi,[42] whereas the parameters of the Brooks–Corey[37] and van Genuchten[38] models were based on the experimental measurements of Reitsma and Kueper.[36]

equilibrium was achieved, while no liquid bridge existed.[7] This extra desaturation has been attributed to the liquid film flow across contact points (usually simulated by spacers in experimental works).[7] The liquid film flow across contact points can play an important role in oil recovery beyond the capillary-gravity equilibrium, as discussed by Dindoruk and Firoozabadi.[8] They studied liquid film flow to find the relationship between capillary number, fracture-liquid permeability, and the shape of the gas–liquid interface. They concluded that the liquid film flow satisfies Darcy's law for the same order of capillary numbers in porous media and also that the liquid bridge interface in a horizontal fracture has a circular shape for this range of capillary numbers.[8]

Discussion on the Stability of a Liquid Bridge Between Matrix Blocks

Since a stable liquid bridge formed in a horizontal fracture between matrix blocks guarantees capillary continuity,[2,4,7,10,13] the stability boundaries of the created liquid bridge need to be addressed.

The maximum stable length of a vertically suspended liquid bridge is controlled by the balance between hydrostatic pressure, which increases with distance from the top of the liquid bridge, and surface tension forces.[44–47] According to the theory proposed by Plateau[48] and Rayleigh,[49] the maximum stable limit of liquid bridge length in the absence of gravity is $l = 2\pi r$, when r is radius of the liquid bridge. The plateau stability limit decreases with an increasing Bond number.[48]

The dynamic and static stability of a liquid bridge is usually studied by using volume or pressure control conditions. Most of these investigations are performed under the microgravity fields between two impermeable solid bodies, such as parallel disks, spherical plate, and spherical–spherical bodies.[41] In these cases, perturbations may be induced by differences between contact areas, solid body rotation on an axially gravitational field and imposing magnetic or electrical fields.[41] In naturally fractured reservoirs, perturbations may be induced by parameters, such as variations in the feeding flux from the top of the bridge, a pressure variation in the fracture, fracture surface characteristics, and fracture geometry and orientation. Here, the complexity of problem becomes evident, and the choice of some assumptions appears to be important for solving this difficult problem.

Summary and Conclusions

Understanding and addressing the specific challenges of fluid flow mechanisms are very important in the prediction and optimization of oil recovery from naturally fractured reservoirs. It is well known that some degree of block-to-block interaction exists, which may affect oil recovery from such reservoirs. This is an important issue that needs to be addressed in fractured reservoir flow modeling.

One of the important physical mechanisms involved in block-to-block interaction is the formation and detachment of liquid bridges. Accurate modeling of the growth and detachment of traveling liquid bridges, which may cause capillary continuity between matrix blocks, remains a controversial topic. In this work, we have presented a mechanistic model that considers the formation, growth, and detachment of pendant liquid elements, perpendicular to a horizontal fracture between porous matrix blocks. The mechanistic model was then coupled with various upscaled fracture capillary pressure models to investigate the formation of liquid bridges. The effect of various fracture capillary pressure models on the critical length of the liquid element was considered. An expression has been obtained that relates the commonly used fracture capillary pressure to the critical length of the liquid element.

A customary assumption in the simulation of naturally fractured reservoirs is zero capillary pressure in the fracture. It was shown that, for zero fracture capillary pressure, liquid bridges between matrix blocks do not form. It was also shown that, when the fracture capillary pressure is a constant value and the threshold Bond number is smaller than 0.25, a liquid bridge is formed that may lead to capillary continuity. For a saturation dependant fracture capillary pressure model, we found that the formation of a liquid bridge is possible for a threshold Bond number of less than 0.5.

It was also shown that, at constant fracture oil saturation (or constant fracture capillary pressure), the critical length of the liquid element decreases when the threshold Bond number increases. This implies a smaller critical length of the liquid element for a higher density difference between the two phases. The results also showed that, at constant fracture oil saturation and high threshold Bond numbers, the critical length of the liquid element tends to zero, implying that a liquid bridge does not form. Conversely, as the threshold Bond number tends to zero, the critical length of the liquid element approaches large values, suggesting that formation of a liquid bridge is possible.

We found that, at a constant threshold Bond number of 0.05, as the wetting phase saturation in the fracture goes immediately above the residual oil saturation, the critical length of the liquid element is above 10 μm, suggesting that a liquid bridge can form for an aperture below this critical value. The results also demonstrated that as the wetting phase saturation approaches one, a fracture capillary pressure model with threshold height results in a finite value for the critical length of the liquid element. On the other hand, a fracture capillary pressure model asymptotically approaching zero capillary pressure, as the fracture wetting phase saturation tends to one, leads to an infinite critical length for the liquid element.

The results show that the threshold Bond number is an important parameter in the formation of liquid bridges. The critical fracture aperture that results in capillary continuity is a strong function of the threshold Bond number. The critical fracture aperture for the formation of liquid bridges can be different in orders of magnitude, depending on the prevailing threshold Bond number. At very low Bond numbers, the critical fracture aperture can be as high as a couple of millimeters; whereas, at high Bond numbers, it can be in the order of micrometers. This highlights the importance of the determination of the threshold Bond number in the investigation of the effect of block-to-block interaction in naturally fractured reservoirs.

Acknowledgments

The final version of this article has significantly benefited from comments by the reviewer. These comments are gratefully acknowledged. The authors

acknowledge useful comments from Ali M. Saidi. The first author is appreciative of the support of his parents, Dariush Dejam and Zahra Fakhari. They have been a source of encouragement and inspiration.

Literature Cited

1. Warren JE, Root PJ. The behavior of naturally fractured reservoirs. *SPE J*. 1963;3:245–255.
2. Saidi AM. *Reservoir Engineering of Fractured Reservoirs-Fundamentals and Practical Aspects*. Paris: Total Edition Press, 1987.
3. Saidi AM, Tehrani DH, Wit K. *Mathematical Simulation of Fractured Reservoir Performance, Based on Physical Model Experiments*. WPC18227 Tenth World Petroleum Congress, September 9-14, 1979, Bucharest, Romania, 225–233.
4. Horie T, Firoozabadi A, Ishimoto K. Laboratory studies of capillary interaction in fracture/matrix systems. *SPE Res Eval Eng*. 1990;5: 353–360.
5. Firoozabadi A, Hauge J. Capillary pressure in fractured porous media. *J Petrol Technol*. 1990;42:784–791.
6. Labastie A. *Capillary Continuity Between Blocks of a Fractured Reservoir*. SPE20515, Paper presented at the SPE Annual Technical Conference and Exhibition, New Orleans, Louisiana, 23–26 September 1990. doi:10.2118/20515-MS.
7. Firoozabadi A, Markeset T. An experimental study of the gas–liquid transmissibility in fractured porous media. *SPE Res Eval Eng*. 1994;9:201–207.
8. Dindoruk B, Firoozabadi A. Liquid film flow in a fracture between two porous blocks. *Phys Fluids*. 1994;6:3861–3869.
9. Firoozabadi A, Markeset T. Laboratory studies in fractured porous media. Part I. Reinfiltration for gas–liquid systems. *In Situ*. 1995;19:1–21.
10. Aspenes E, Ersland G, Graue A, Stevens J, Baldwin BA. Wetting phase bridges establish capillary continuity across open fractures and increase oil recovery in mixed-wet fractured chalk. *Transport Porous Med*. 2008;74:35–47.
11. Hoteit H, Firoozabadi A. Numerical modeling of two-phase flow in heterogeneous permeable media with different capillarity pressures. *Adv Water Resour*. 2008;31:56–73.
12. Hoteit H, Firoozabadi A. An efficient numerical model for incompressible two-phase flow in fractured media. *Adv Water Resour*. 2008;31:891–905.
13. Sajjadian VA, Danesh A, Tehrani DH. *Laboratory Studies of Gravity Drainage Mechanism in Fractured Carbonate Reservoir-Capillary Continuity*. SPE49497, Paper presented at the Abu Dhabi International Petroleum Exhibition and Conference, Abu Dhabi, United Arab Emirates, 11–14 November 1998.
14. Ghezzehei TA, Or D. Liquid fragmentation and intermittent flow regimes in unsaturated fractured porous media. *Water Resour Res*. 2005;41:W12406.
15. Or D, Ghezzehei TA. Traveling liquid bridges in unsaturated fractured porous media. *Transport Porous Media*. 2007;68:129–151.
16. Prazak J, Sir M, Kubik F, Tywoniak J, Zarcone C. Oscillation phenomena in gravity-driven drainage in coarse porous-media. *Water Resour Res*. 1992;28:1849–1855.
17. Hoffman RL. A study of the advancing interface. I. Interface shape in liquid-gas systems. *J Colloid Interface Sci*. 1975;50:228.
18. Seaver AE, Berg JC. Spreading of a droplet on a solid surface. *J Appl Polym Sci*. 1994;52:431–435.
19. Sikalo S, Wilhelm HD, Roisman IV, Jakirlic S, Tropea C. Dynamic contact angle of spreading droplets: experiments and simulations. *Phys Fluids*. 2005;17:062103.
20. Wilson SDR. The slow dripping of viscous fluid. *J Fluid Mech*. 1988;190:561–570.
21. Matta JE, Tytus RP. Liquid stretching using a falling cylinder. *J Non-Newton Fluid Mech*. 1990;35:215–229.
22. Ferguson J, Hudson NE, Odriozola MA. The interpretation of transient extensional viscosity data. *J Non-Newton Fluid Mech*. 1997;68:241–257.
23. Zhou D, Blunt MJ, Orr FM. Hydrocarbon drainage along corners of noncircular capillaries. *J Colloid Interface Sci*. 1997;187:11–21.
24. Green DW, Willhite GP. *Enhanced Oil Recovery*. Society of Petroleum Engineers, 1998.
25. Zhou D, Blunt MJ. Wettability effects in three-phase gravity drainage. *J Petrol Sci Eng*. 1998;20:203–211.
26. Laroche C, Vizika O, Kalaydjian F. *Network Modeling to Predict the Effect of Wettability Heterogeneities on Multiphase Flow*. SPE56674, Paper presented at the SPE Annual Technical Conference and Exhibition, Houston, Texas, 3–6 October 1999.
27. Hui MH, Blunt MJ. Effects of wettability on three-phase flow in porous media. *J Phys Chem B*. 2000;104:3833–3845.
28. Lego M, Araujo M. Threshold pressure in capillaries with polygonal cross section. *J Colloid Interface Sci*. 2001;243:219–226.
29. Weitz DA, Stokes JP, Ball RC, Kushnick AP. Dynamic capillary pressure in porous media: origin of the viscous-fingering length scale. *Phys Rev Lett*. 1987;59:2967–2970.
30. de Gennes PG. Dynamic capillary pressure in porous media *Europhys Lett*. 1988;5:689–691.
31. Bico J, Quere D. Falling slugs. *J Colloid Interface Sci*. 2001;243: 262–264.
32. Kueper BH, McWhorter DB. The behavior of dense, non-aqueous phase liquids in fractured clay and rock. *J Ground Water*. 1991;29:716–728.
33. Streeter VL, Wylie EB, Bedford KW. *Fluid Mechanics*. McGraw-Hill, 1998.
34. Rossen RH, Shen EI. Simulation of gas–oil drainage and water/oil imbibition in naturally fractured reservoirs. *Trans AIME*. 1989;287:464–470.
35. Quandalle P, Sabathier JC. Typical features of a new multiphase reservoir simulator. *SPE Res Eval Eng*. 1989;4:475–480.
36. Reitsma S, Kueper BH. Laboratory measurement of capillary pressure-saturation relationships in a rock fracture. *Water Resour Res*. 1994;30:865–878.
37. Brooks RH, Corey AT. *Hydraulic Properties of Porous Media*. Hydrology Paper No. 3, Fort Collins: Civil Engineering Department, Colorado State University, 1964.
38. van Genuchten MT. A closed form equation for predicting the hydraulic conductivity of unsaturated soils. *Soil Sci Am J*. 1980;44: 892–898.
39. Mualem Y. A new model for predicting the hydraulic conductivity of unsaturated porous media. *Water Resour Res*. 1976;12:513–522.
40. Dindoruk B, Firoozabadi A. Computation of gas–liquid drainage in fractured porous media recognizing fracture liquid flow. *J Can Petrol Technol*. 1995;34:39–49.
41. Kralchevsky PA, Nagayama K. *Studies in Interface Science: Particles at Fluid Interfaces and Membranes*. Elsevier, 2001.
42. Tan JCT, Firoozabadi A. *Dual-Porosity Simulation Incorporating Reinfiltration and Capillary Continuity Concepts: Part I—Single Grid Cell*. SPE29113, Paper presented at the SPE Reservoir Simulation Symposium, San Antonio, Texas, 12–15 February 1995.
43. Firoozabadi A, Katz DL, Soroosh H, Sajjadian VA. Surface tension of reservoir crude-oil/gas systems recognizing the asphalt in the heavy fraction. *SPE J*. 1988;3:134–145.
44. Martinez I. *Stability of Axisymmetric Liquid Bridges*. Proceedings of the fourth European Symposium on Materials Sciences under Microgravity, Madrid, Spain, 5–8 April 1983 (ESA SP-191-June 1983).
45. Rivas D, Mesenguer J. One-dimensional self-similar solution of the dynamics of axisymmetric slender liquid bridges. *J Fluid Mech*. 1983;138:417–429.
46. Eggers J, Dupont TF. Drop formation in a one-dimensional approximation of the Navier–Stokes equation. *J Fluid Mech*. 1993;262:205–221.
47. Eggers J, Villermaux E. Physics of liquid jets. *Rep Prog Phys*. 2007;71:036601.
48. Plateau JAF. *Experimental and Theoretical Researches on the Figures of Equilibrium of a Liquid Mass Withdrawn from the Action of Gravity*. Annual Report, Smithsonian Institute. 1863:207–285.
49. Rayleigh L. *On the Instability of Jets*. Proceedings of the London Mathematical Society. 1878;s1–10:4–13. doi:10.1112/plms/s1-10.1.4.

Appendix

The force balance equation (Eq. 6) can be written in dimensionless form as[20]:

$$\frac{\partial A_D}{\partial t_D} - \delta A_D^{1/2} = -\frac{1}{3}\tau_D \tag{A1}$$

where $t_D = t/(\mu A_0/\rho g Q)^{1/2}$, $\tau_D = \tau/(\mu A_0/\rho g Q)^{1/2}$, $A_D = A/A_0$, and $\delta = (\pi/9\mu\rho g Q)^{1/2}$.

The related initial condition in dimensionless form is given by:

$$A_D = 1 \quad @ \; t_D = \tau_D. \tag{A2}$$

The analytical solution for the differential equation given by Eq. A1, subject to the initial condition (Eq. A2), is given by[20]:

$$t_D = \tau_D + \frac{2}{\delta}\left[A_D^{1/2} - 1 + \frac{\tau_D}{3\delta}\ln\left(\frac{3\delta A_D^{1/2} - \tau_D}{3\delta - \tau_D}\right)\right]. \tag{A3}$$

If we set $A_D = 0$, it is possible to obtain the relation between t_D and τ_D when the cross-sectional area goes to zero. Using the critical values for t_D and τ_D as t_{DC} and τ_{DC}, respectively, we have[20]:

$$t_{Dc} = \tau_{Dc} - \frac{2}{\delta}\left[1 + \frac{\tau_{Dc}}{3\delta}\ln\left(\frac{\tau_{Dc} - 3\delta}{\tau_{Dc}}\right)\right]. \tag{A4}$$

Since Q is constant and the liquid is incompressible when the cross-sectional area goes to zero, its length approaches infinity, implying that the rate of movement of a liquid particle, $d\tau_{Dc}/dt_{Dc}$ approaches infinity. In other words, $dt_{Dc}/d\tau_{Dc} \rightarrow 0$. This condition results in the following implicit relation between τ_{Dc} and δ:

$$\tau_{Dc} = \frac{2}{\delta}\left[\frac{\tau_{Dc}}{3\delta}\ln\left(\frac{\tau_{Dc} - 3\delta}{\tau_{Dc}}\right) + \frac{\tau_{Dc}}{\tau_{Dc} - 3\delta}\right]. \tag{A5}$$

Manuscript received Aug. 21, 2009, and revision received Mar. 15, 2010.